PROTEIN STRUCTURE REPORT

Solution structure of the PHD finger from the human KIAA1045 protein

Kazuhide Miyamoto,* Ayumi Yamashita, and Kazuki Saito

Department of Pharmaceutical Health Care, Faculty of Pharmaceutical Sciences, Himeji Dokkyo University, Hyogo, Japan

Received 14 November 2017; Accepted 6 February 2018
DOI: 10.1002/pro.3389
Published online 12 February 2018 proteinscience.org

Abstract: Cross-brace structural motifs are required as a scaffold to design artificial RING fingers (ARFs) that function as ubiquitin ligase (E3) in ubiquitination and have specific ubiquitin-conjugating enzyme (E2)-binding capabilities. The Simple Modular Architecture Research Tool database predicted the amino acid sequence 131–190 (KIAA1045ZF) of the human KIAA1045 protein as an unidentified structural region. Herein, the stoichiometry of zinc ions estimated spectrophotometrically by the metallochromic indicator revealed that the KIAA1045ZF motif binds to two zinc atoms. The structure of the KIAA1045ZF motif bound to the zinc atoms was elucidated at the atomic level by nuclear magnetic resonance. The actual structure of the KIAA1045ZF motif adopts a C_4HC_3-type PHD fold belonging to the cross-brace structural family. Therefore, the utilization of the KIAA1045ZF motif as a scaffold may lead to the creation of a novel ARF.

Keywords: cross-brace structure; PHD finger; RING finger; zinc finger; ubiquitination; artificial RING finger

Introduction

The cross-brace structure is a common zinc-binding motif among the RING,[1] PHD,[2] FYVE,[3] and ZZ[4] fingers. Besides this motif, each finger is unique with a specific biological function.[4] For example, the RING fingers are involved in a pathway of protein ubiquitination and function as ubiquitin ligase (E3).[5] They specifically bind to ubiquitin-conjugating enzyme (E2), and transfer the activated ubiquitin (Ub) to lysine residues of substrates.[6,7] The helical region of the RING fingers is an active site for their specific E2-binding capabilities for ubiquitination.[1,8,9] In contrast, the PHD, FYVE, and ZZ fingers cannot perform protein ubiquitination because they lack a functional helix, although they sometimes have a short helix structure in a turn conformation.[2,3,10] In a previous study, we have developed the "α-helical region substitution" method for creating an artificial RING finger (ARF), which possesses E3 activity and specific E2-binding capabilities. Utilizing ARFs enables the quantitative detection of E2 activities in ubiquitination.[11] Because E2 activities are associated with various cancers, such as leukemia[12] and lung[13] and breast[14] cancers, the ARF methodology could be used for developing novel diagnostic techniques for cancer. An ARF is engineered by transplanting a helical region (active site) of one RING finger into other cross-brace structures.[15] In other words, the method of α-helical region substitution confers E3 activity of a RING finger onto the other

Additional Supporting Information may be found in the online version of this article.

Grant sponsor: Scientific Research (KAKENHI 17K05942) and the Nakatani Foundation.

*Correspondence to: Kazuhide Miyamoto, Department of Pharmaceutical Health Care, Faculty of Pharmaceutical Sciences, Himeji Dokkyo University, Hyogo 670-8524, Japan. E-mail: miyamoto@himeji-du.ac.jp

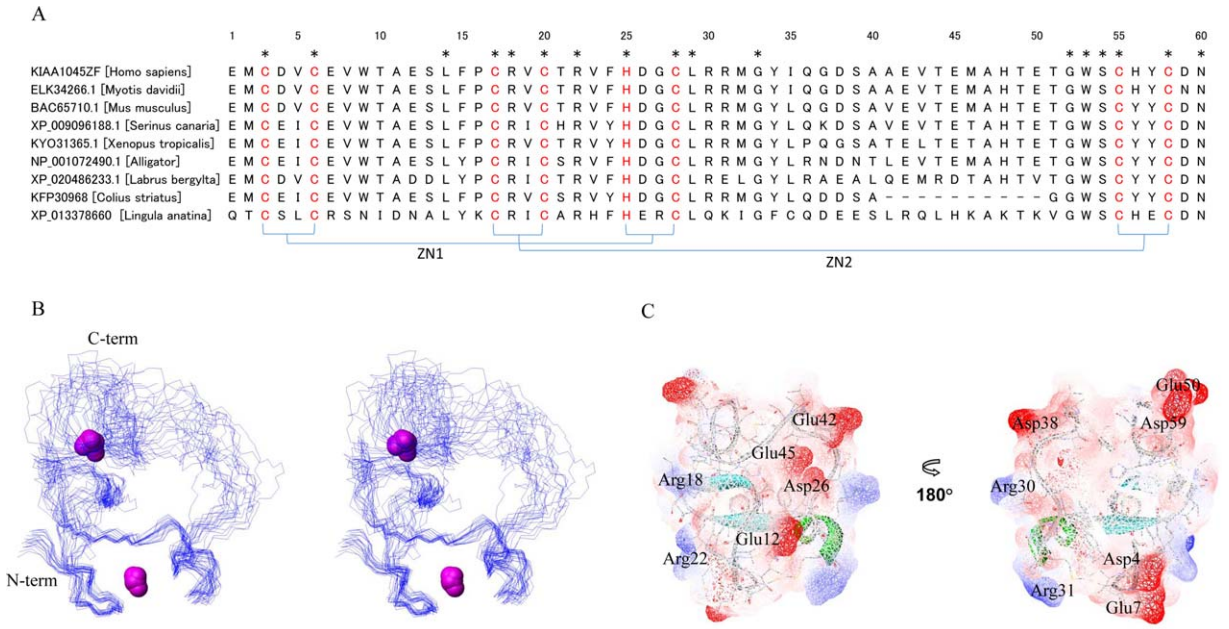

Figure 1. (A) Sequence alignment of the KIAA1045ZF motif from the human KIAA1045 protein. ZN1 and ZN2 indicate the two zinc-binding sites with a cross-brace fashion. The zinc ligands are shown in red. The stars indicate the completely conserved residues among homologs. (B) Stereoview showing the trace of the backbone for ensemble structures of the 20 lowest energy conformers. The zinc atoms are depicted in magenta. (C) Surface representation and ribbon diagram of the KIAA1045ZF motif illustrating the side chains. The Connolly surface is shown with the electrostatic potential (blue, positive; red, negative). The α-helical and β-sheet regions are shown in green and blue, respectively.

cross-brace structures. To extend this method to various cross-brace structures, we need to unravel their atomic structures to identify appropriate positions for the grafting of active sites. The human KIAA1045 protein comprises 400 amino acids and is considered to be a coding sequence of an unidentified gene.[16] The Universal Protein Resource (UniProt) search provides the annotation (Q9UPV7) of a PHD-type zinc finger on the amino acid sequence 131–190 (KIAA1045ZF) of the human KIAA1045 protein, however it is predicted to have an unidentified structural region as per the Simple Modular Architecture Research Tool (SMART) database query/search. The KIAA1045ZF motif is the fascinating domain, and thus, we investigated the solution structure of the KIAA1045ZF motif using nuclear magnetic resonance (NMR). There is a challenge in predicting the structure via the sequence database regarding the KIAA1045ZF motif. However, structural analysis demonstrated that the actual structure of the KIAA1045ZF motif adopts a PHD fold in a cross-brace fashion.

Methods

Peptide synthesis

The KIAA1045ZF motif was constructed using the domain positioned at 131–190 of the human KIAA1045 protein and renumbered as 1–60 [Fig. 1(A)]. Using the standard F-moc solid-phase method, the ^{13}C and ^{15}N-labeled KIAA1045ZF motif was uniformly synthesized using chemicals for peptide assembly. After cleavage with trifluoroacetic acid, the peptide was purified using HPLC with a Shimpack C18 column (Shimadzu Corp.). Peptide purity was >95% and the molecular mass was determined using MALDI-TOF MS on the Shimadzu AXIMA-TOF2. The compact KIAA1045ZF motif can be stored as a powder. The peptide was dissolved in 0.33 mL of 8 M guanidine-HCl, and the solution was dialyzed against degassed solution [20 mM Tris-HCl (pH 6.9), 50 mM NaCl, 1 mM dithiothreitol, and 50 μM $ZnCl_2$] overnight at 4°C using the Slide-A-Lyzer Dialysis Cassette (PIERCE).[17,18]

Estimation of the amount of released zinc ions

The concentration of the KIAA1045ZF motif was spectrophotometrically determined using the Bradford method. Zinc ions were released from the KIAA1045ZF motif by cysteine modification of *p*-hydroxymercuribenzoic acid (PHMB). The Zn^{2+}–PAR_2 complex was formed using the metallochromic indicator 4-(2-pyridylazo)resorcinol (PAR). Absorbance values of the complex at 20°C were recorded at 500 nm. The amount of zinc ions was estimated based on the equation $A = \varepsilon cl$, where the molar absorptivity (ε) is 6.6×10^4 M^{-1} cm^{-1}, the cell length (l) is 1.0 cm, and c represents the molecular concentration. The stoichiometry of released zinc ions (zinc:KIAA1045ZF) was calculated using the

amount of released zinc ions and the KIAA1045ZF motif.[19–21]

NMR spectroscopy

The KIAA1045ZF motif (1 mM) was dissolved in $^1H_2O/^2H_2O$ (9:1) in 20 mM Tris-d_{11}-HCl buffer (pH 6.9) (C/D/N Isotopes, Canada) containing 50 mM NaCl, 1 mM 1,4-DL-dithiothreitol-d_{10}, and 50 μM $ZnCl_2$.[22,23] NMR experiments at 20°C were performed on the Bruker AVANCE 500 MHz equipped with a cryogenic probe and AVANCE 800 spectrometer using the WATERGATE pulse sequence.[24] The three-dimensional ^{15}N- and ^{13}C-edited NOESY spectra were measured using mixing times of 80 ms for structure calculations. The backbone was assigned using the standard triple-resonance experiments.[25] Resonance assignments of the side chains were performed using HBHACONH, HCCCONNH, CCCONNH, HCCH-TOCSY, and HCCH-COSY spectra, whereas those of the aromatic rings were achieved using a combination of HCCH-COSY and ^{13}C-edited NOESY spectra. The spectra were processed with the program NMRPipe[26] and spectral analysis was performed using NMRView.[27]

Structure calculation

Peak lists for each of the ^{15}N- and ^{13}C-edited NOESY spectra were generated using the functions of NMRView. Stereospecific assignments of the methyl groups of Val and Leu were made when their NOE patterns were distinct from each other. Automated NOE cross-peak assignments and structure calculations with torsion angle dynamics were performed using the program CYANA 2.1.[28] For structure calculations, 100 randomized conformers were generated and the standard CYANA-simulated annealing protocol was utilized with 10,000 torsion angle dynamic steps per conformer. NOEs for the hydrogen bond were not observed. To experimentally elucidate the structure of KIAA1045ZF based on NOE restraints, dihedral angles constraints were not used for the calculations. For energy minimization, 20 conformers with the lowest CYANA target function values were subjected to the Smart Minimizer algorithm (Max steps 200, root-mean-square (RMS) gradient 0.01) in the program Discovery Studio 2.1 (Accelrys Software).[15] For tetrahedral zinc coordination, the distance constraints ($Zn–S_\gamma$, $Zn–C_\beta$, and $S_\gamma–S_\gamma$ for Cys, and $Zn\text{-}N_{\delta1}$ and $S_\gamma\text{-}N_{\delta1}$ for His) with force constants of 500 kcal mol^{-1} $Å^{-1}$ were added in the peak lists.[29,30] The resulting structures were validated using the PROCHECK-NMR.[31] The 20 conformers were fitted using the program MOLMOL.[32] The Connolly surface of the structure was calculated using Discovery Studio 2.1.

Table I. *Summary of Structure Statistics of the KIAA1045ZF Motif*[a]

NOE upper distance restraints	
Total	645
Short-range ($\|i-j\|=1$)	427
Medium range ($1<\|i-j\|<5$)	74
Long rage ($\|i-j\|\geq5$)	144
CYANA target function value	$0.07Å^2$
Distance constraints violations	
Number > 0.1 Å	0
Maximum	0.03Å
PROCHECK Ramachandran plot analysis[b]	
Residues in most favored regions	63.1%
Residues in additionally allowed regions	28.7%
Residues in generously allowed regions	6.7%
Residues in disallowed regions	1.5%
RMS deviation to the average coordinates[b]	
Backbone atoms	0.80Å
Heavy atoms	1.35Å

[a] Except for the number of constraints, average values given for the set of 20 conformers with the lowest energy value.
[b] The values were calculated for residues 2–9, 15–17, 20–32, and 54–58.

Results and Discussion

The KIAA1045ZF motif binds two zinc atoms

The concentration of the KIAA1045ZF motif was 2.7 μM and the absorbance value at 500 nm for the Zn^{2+}–PAR_2 complex was 0.35. The calculated concentration of the zinc ions was 5.3 μM. Therefore, the zinc:KIAA1045ZF ratio was 1.96 at 20°C, indicating that the KIAA1045ZF motif binds to two zinc atoms.

NMR assignments and overall structure

Resonance assignments of the backbone were completely assigned except for the amide protons of the residues Glu1 and Asn60. The C_β atoms of the residues Cys3, Cys6, Cys17, Cys20, Cys28, Cys55, and Cys58 were between 27.0 and 32.0 ppm, showing that they are zinc-binding ligands.[33] The His25 residue forms an $N_{\varepsilon2}$-H tautomer as a possible zinc-binding ligand because its $C_{\delta2}$ atom is less than 122 ppm.[34] The residues Cys3, Cys6, His25, and Cys28 were clustered to form one of the two zinc-binding sites supported by their NOE connectivities. All the ligating residues were completely conserved among the homologs of the KIAA1045ZF motif [Fig. 1(A)]. The solution structure of the KIAA1045ZF motif was calculated using CYANA[28] and Discovery Studio 2.1.[15] The superimposition of the backbone of the 20 lowest energy structures of the KIAA1045ZF motif is shown in Figure 1(B). The structural statistics for the 20 conformers are summarized in Table I. The well-ordered region (Met2–Trp9, Phe15–Cys17, Cys20–Met32, and Ser54–Cys58) are superimposed over the backbone (N, C^α, and C′) and non-hydrogen atoms, with RMS deviations (RMSD) of 0.80 Å and 1.35 Å, respectively. The long loop exits in the region

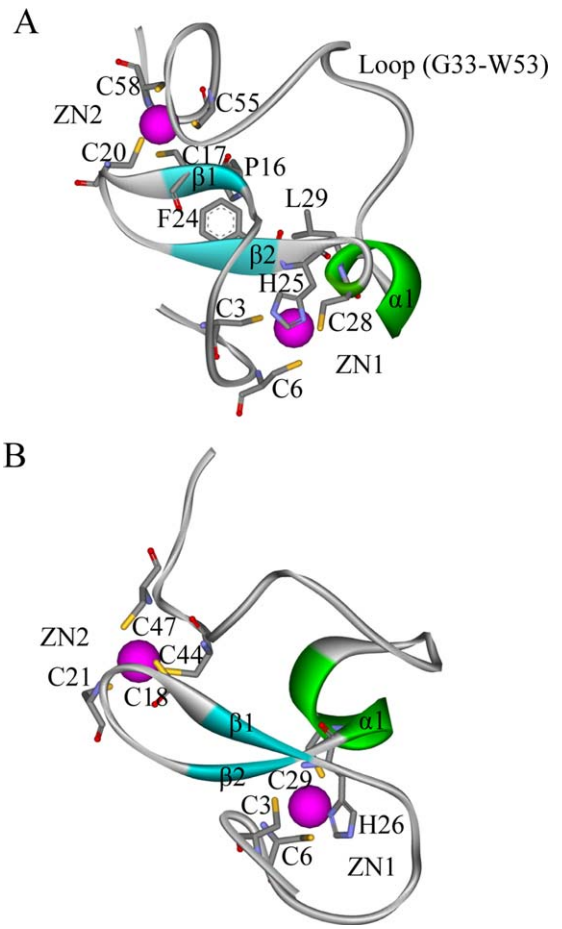

Figure 2. Structural comparisons with the KIAA1045ZF motif. Ribbon diagrams of (A) the lowest energy structure of the KIAA1045ZF motif showing the heavy atoms of the side chains of the hydrophobic core residues and the zinc-binding ligands. (B) The WSTF PHD structure, showing the zinc-binding ligands. The zinc atoms, β strands, and α-helix are shown in magenta, blue, and green, respectively.

of the residues Gly33–Trp53. PROCHECK-NMR[31] analysis formed a Ramachandran plot, i.e., 91.8% of the well-ordered region was in the most favored and additionally allowed regions. The Connolly surface of the lowest energy structure was calculated as solvent contact areas that were traced out by a probe (water) molecule of radius 1.4 Å using Discovery Studio 2.1 [Fig. 1(C)].[35] The residues Glu12, Asp26, Glu42, and Glu45 formed a highly acidic surface. NMR data indicated that the KIAA1045ZF motif possesses one α-helix and one antiparallel β sheet (α1: Leu29–Met32, β1: Pro16–Cys17, β2: Val23–Phe24) [Fig. 2(A)]. The zinc-binding fashion of the KIAA1045ZF motif was a C_4HC_3-type in a cross-brace arrangement. The zinc atoms contribute to the formation of the ligation pattern (CCHC and CCCC), separated by β1 and β2. The residues Pro16, Phe24, and Leu29 contribute to the formation of the hydrophobic core for proper folding. Taken together, our findings indicate that the structure of the KIAA1045ZF motif adopts a compact zinc-binding fold in a cross-braced fashion.

Comparison with other PHD structures

The KIAA1045ZF motif was predicted to be an unidentified structural domain by the SMART database query. It seems that the prediction of the secondary structures of the cross-braced domains via the sequence database is a challenge due to few components for building up their secondary structures. However, we found that the C_4HC_3-type zinc-binding pattern of the KIAA1045ZF motif is in agreement with that of the PHD fold.[36] The typical PHD structure from the human Williams-Beuren Syndrome Transcription Factor (WSTF) protein[2] is shown in Figure 2(B). The data showed that the structure is a cross-braced zinc-binding arrangement and has antiparallel β-sheet and α-helical structures. Thus, the structure of the KIAA1045ZF motif evidently adopts the PHD fold. Pro16 was in cis-conformation, which was confirmed by chemical shift differences between C_β and C_γ[37] and NOE pattern between the $H_\alpha(i-1)$ and $H_\delta(i)$ protons.[38] In the cis-conformation of X-Pro16, $H_\alpha(i-1)$ and $H_\alpha(i)$ protons were spatially close to each other. Pro16 promotes the bending of the antiparallel β-sheet, although the structurally equivalent Pro residue does not exist in the WSTF PHD. Thus, Pro16 of the KIAA1045ZF motif leads to the formation of a structure distinct from that of the WSTF PHD. The PHD fingers from various proteins play roles as phosphoinositide (PtdInsP)-binding modules. The WSTF PHD finger specifically binds to phosphatidylinositol 3-phosphate and phosphatidylinositol 5-phosphate.[39] The positively charged residues (Lys4 and Lys23) around the β2 strand of the WSTF PHD finger are essential keys for PtdInsP-binding capabilities (Supporting Information Fig. S1A). As for the structure of the KIAA1045ZF motif, the structurally equivalent positive residues (Arg18 and Arg22) were completely conserved among homologs, and they existed around the β2 strand as shown in Supporting Information Figure S1B. Therefore, it is tempting to speculate that the KIAA1045ZF motif possesses specific PtdInsP-binding capabilities, which are involved in signal transduction pathways.

Cross-brace structure for engineering an ARF

Utilizing ARFs allows for the simplified detection of E2 activities in ubiquitination reactions and leads to the assessment of pathological conditions of acute promyelocytic leukemia-derived NB4 cells.[11,12] When engineering ARFs, the active site of the RING finger is transplanted into other cross-brace structures.

Because the KIAA1045ZF motif adopts the cross-brace structure, it is utilized as a scaffold for the ARF methodology. If the loop (G33-W53) of the KIAA1045ZF motif is replaced with the helical region (active site) of the EL5 RING finger, the resulting ARF might function as an E3 ligase. In

this work, we unraveled the position and range of the loop (G33-W53) of the KIAA1045ZF motif at the atomic level, leading to the design for engineering a novel ARF. It was found that eight residues of Cys and His are the zinc ligands for forming C_4HC_3 zinc coordination. Given that ARFs could be clinically used as a cancer diagnostic technique, aspects such as easy handling, transportability, and minimal/no lot-to-lot variations are desirable when designing ARFs. Thus, it is inevitably needed to make the compact motif of the cross-brace zinc finger as a scaffold for ARF. In this study, we have succeeded in making the functional compact construct for the KIAA1045ZF motif as a 60-mer peptide. The present compact molecular size of the KIAA1045ZF motif enabled the use of the standard peptide synthesis. The knowledge obtained in this study is useful, when we utilize the KIAA1045ZF motif as a scaffold for ARF. Therefore, the present research lends credence to the use of ARFs. Further studies of ubiquitination assay and ARF structures are needed for comprehensively understanding the structure-function relationship of ARFs.

In conclusion, this work provided the first documented structural study of the zinc finger of the human KIAA1045 protein. We revealed that the zinc finger adopts the PHD structure as a scaffold for ARFs.

Protein data bank accession number

The atomic coordinates (code 5XHT) have been deposited in the Protein Data Bank, Research Collaboratory for Structural Bioinformatics.

Acknowledgments

The authors would like to thank Dr. Yoshitsugu Shiro, RIKEN SPring-8 Center, for the NMR instrumentation.

Author Contributions

K.M. designed this study, drafted the main manuscript, and prepared all the figures. All the authors performed the experiments and reviewed the manuscript.

Conflict of Interest

The authors declare no competing financial interests.

References

1. Zheng N, Wang P, Jeffrey PD, Pavletich NP (2000) Structure of a c-Cbl-UbcH7 complex: RING domain function in ubiquitin-protein ligases. Cell 102:533–539.
2. Pascual J, Martinez-Yamout M, Dyson HJ, Wright PE (2000) Structure of the PHD zinc finger from human Williams-Beuren syndrome transcription factor. J Mol Biol 304:723–729.
3. Misra S, Hurley JH (1999) Crystal structure of a phosphatidylinositol 3-phosphate-specific membrane-targeting motif, the FYVE domain of Vps27p. Cell 97:657–666.
4. Legge GB, Martinez-Yamout MA, Hambly DM, Trinh T, Lee BM, Dyson HJ, Wright PE (2004) ZZ domain of CBP: an unusual zinc finger fold in a protein interaction module. J Mol Biol 343:1081–1093.
5. Joazeiro CA, Weissman AM (2000) RING finger proteins: mediators of ubiquitin ligase activity. Cell 102: 549–552.
6. Lorick KL, Jensen JP, Fang S, Ong AM, Hatakeyama S, Weissman AM (1999) RING fingers mediate ubiquitin-conjugating enzyme (E2)-dependent ubiquitination. Proc Natl Acad Sci U S A 96:11364–11369.
7. Weissman AM (2001) Themes and variations on ubiquitylation. Nat Rev Mol Cell Biol 2:169–178.
8. Brzovic PS, Rajagopal P, Hoyt DW, King MC, Klevit RE (2001) Structure of a BRCA1-BARD1 heterodimeric RING-RING complex. Nat Struct Biol 8:833–837.
9. Katoh S, Tsunoda Y, Murata K, Minami E, Katoh E (2005) Active site residues and amino acid specificity of the ubiquitin carrier protein-binding RING-H2 finger domain. J Biol Chem 280:41015–41024.
10. Scheel H, Hofmann K (2003) No evidence for PHD fingers as ubiquitin ligases. Trends Cell Biol 13:285–287. author reply 287–288.
11. Miyamoto K, Sumida M, Yuasa-Sunagawa M, Saito K (2017) Highly sensitive detection of E2 activity in ubiquitination using an artificial RING finger. J Pept Sci 23:222–227.
12. Takenokuchi M, Miyamoto K, Saigo K, Taniguchi T (2015) Bortezomib causes ER stress-related death of acute promyelocytic leukemia cells through excessive accumulation of PML–RARA. Anticancer Res 35:3307–3316.
13. van Ree JH, Jeganathan KB, Malureanu L, van Deursen JM (2010) Overexpression of the E2 ubiquitin-conjugating enzyme UbcH10 causes chromosome missegregation and tumor formation. J Cell Biol 188:83–100.
14. Wu X, Zhang W, Font-Burgada J, Palmer T, Hamil AS, Biswas SK, Poidinger M, Borcherding N, Xie Q, Ellies LG, Lytle NK, Wu LW, Fox RG, Yang J, Dowdy SF, Reya T, Karin M (2014) Ubiquitin-conjugating enzyme Ubc13 controls breast cancer metastasis through a TAK1-p38 MAP kinase cascade. Proc Natl Acad Sci U S A 111:13870–13875.
15. Miyamoto K (2014) Structural model of ubiquitin transfer onto an artificial RING finger as an E3 ligase. Sci Rep 4:6574.
16. Kikuno R, Nagase T, Ishikawa K, Hirosawa M, Miyajima N, Tanaka A, Kotani H, Nomura N, Ohara O (1999) Prediction of the coding sequences of unidentified human genes. XIV. The complete sequences of 100 new cDNA clones from brain which code for large proteins in vitro. DNA Res 6:197–205.
17. Miyamoto K, Togiya K (2010) The creation of the artificial RING finger from the cross-brace zinc finger by alpha-helical region substitution. Biochem Biophys Res Commun 394:972–975.
18. Miyamoto K (2012) Ubiquitination of an artificial RING finger without a substrate and a tag. J Pept Sci 18:135–139.
19. Hunt JB, Neece SH, Schachman HK, Ginsburg A (1984) Mercurial-promoted Zn2+ release from Escherichia coli aspartate transcarbamoylase. J Biol Chem 259:14793–14803.

20. Hunt JB, Neece SH, Ginsburg A (1985) The use of 4-(2-pyridylazo)resorcinol in studies of zinc release from Escherichia coli aspartate transcarbamoylase. Anal Biochem 146:150–157.
21. Shang Z, Liao YD, Wu FY, Wu CW (1989) Zinc release from Xenopus transcription factor IIIA induced by chemical modifications. Biochemistry 28:9790–9795.
22. Miyamoto K, Togiya K, Kitahara R, Akasaka K, Kuroda Y (2010) Solution structure of LC5, the CCR5-derived peptide for HIV-1 inhibition. J Pept Sci 16: 165–170.
23. Miyamoto K, Togiya K (2011) Solution structure of LC4 transmembrane segment of CCR5. PLoS One 6:e20452.
24. Piotto M, Saudek V, Sklenar V (1992) Gradient-tailored excitation for single-quantum NMR spectroscopy of aqueous solutions. J Biomol NMR 2:661–665.
25. Clore GM, Gronenborn AM (1994) Multidimensional heteronuclear nuclear magnetic resonance of proteins. Methods Enzymol 239:349–363.
26. Delaglio F, Grzesiek S, Vuister GW, Zhu G, Pfeifer J, Bax A (1995) NMRPipe: a multidimensional spectral processing system based on UNIX pipes. J Biomol NMR 6:277–293.
27. Johnson BA (2004) Using NMRView to visualize and analyze the NMR spectra of macromolecules. Methods Mol Biol 278:313–352.
28. Guntert P (2004) Automated NMR structure calculation with CYANA. Methods Mol Biol 278:353–378.
29. Wang B, Alam SL, Meyer HH, Payne M, Stemmler TL, Davis DR, Sundquist WI (2003) Structure and ubiquitin interactions of the conserved zinc finger domain of Npl4. J Biol Chem 278:20225–20234.
30. Tamames B, Sousa SF, Tamames J, Fernandes PA, Ramos MJ (2007) Analysis of zinc-ligand bond lengths in metalloproteins: trends and patterns. Proteins 69: 466–475.
31. Laskowski RA, Rullmannn JA, MacArthur MW, Kaptein R, Thornton JM (1996) AQUA and PROCHECK-NMR: programs for checking the quality of protein structures solved by NMR. J Biomol NMR 8:477–486.
32. Koradi R, Billeter M, Wuthrich K (1996) MOLMOL: a program for display and analysis of macromolecular structures. J Mol Graph 14:51–55. 29–32.
33. Kornhaber GJ, Snyder D, Moseley HN, Montelione GT (2006) Identification of zinc-ligated cysteine residues based on 13Calpha and 13Cbeta chemical shift data. J Biomol NMR 34:259–269.
34. Sudmeier JL, Bradshaw EM, Haddad KE, Day RM, Thalhauser CJ, Bullock PA, Bachovchin WW (2003) Identification of histidine tautomers in proteins by 2D 1H/13C(delta2) one-bond correlated NMR. J Am Chem Soc 125:8430–8431.
35. Connolly ML (1983) Solvent-accessible surfaces of proteins and nucleic acids. Science 221:709–713.
36. Capili AD, Schultz DC, Rauscher IF, Borden KL (2001) Solution structure of the PHD domain from the KAP-1 corepressor: structural determinants for PHD, RING and LIM zinc-binding domains. EMBO J 20:165–177.
37. Schubert M, Labudde D, Oschkinat H, Schmieder P (2002) A software tool for the prediction of Xaa-Pro peptide bond conformations in proteins based on 13C chemical shift statistics. J Biomol NMR 24:149–154.
38. Wüthrich K (1986) NMR of proteins nucleic acids. New York: John Wiley.
39. Gozani O, Karuman P, Jones DR, Ivanov D, Cha J, Lugovskoy AA, Baird CL, Zhu H, Field SJ, Lessnick SL, Villasenor J, Mehrotra B, Chen J, Rao VR, Brugge JS, Ferguson CG, Payrastre B, Myszka DG, Cantley LC, Wagner G, Divecha N, Prestwich GD, Yuan J (2003) The PHD finger of the chromatin-associated protein ING2 functions as a nuclear phosphoinositide receptor. Cell 114:99–111.